

HOSTED BY



Contents lists available at ScienceDirect

Journal of King Saud University – Science

journal homepage: [www.sciencedirect.com](http://www.sciencedirect.com)

Original article

# Trisodium citrate as a potential and eco-friendly corrosion inhibitor of copper in potable water



Ramasamy Sudhakaran <sup>a</sup>, Thiagarajan Deepa <sup>b</sup>, Munusamy Thirumavalavan <sup>c</sup>, Sharmila Queenthy Sabarimuthu <sup>c</sup>, Sellamuthu Babu <sup>a</sup>, Thayuman Asokan <sup>a</sup>, Pandian Bothi Raja <sup>d</sup>, Natarajan Arumugam <sup>e,\*</sup>, Karthikeyan Perumal <sup>f</sup>, Sinouvassane Djearamane <sup>g,h</sup>, Lai-Hock Tey <sup>h,\*</sup>, Saminathan Kayarohanam <sup>i</sup>

<sup>a</sup> PG & Research Department of Chemistry, Government Arts College, Affiliated to Bharathidasan University, Tiruchirappalli 620 022, Tamil Nadu, India

<sup>b</sup> PG & Research Department of Chemistry, Government Arts College (Autonomous), Affiliated to Bharathidasan University, Karur 639 005, Tamil Nadu, India

<sup>c</sup> Department of Chemistry, Saveetha Engineering College, Saveetha Nagar, Thandalam, Chennai 602105, Tamil Nadu, India

<sup>d</sup> School of Chemical Sciences, Universiti Sains Malaysia, 11800 Penang, Malaysia

<sup>e</sup> Department of Chemistry, College of Science, King Saud University, P.O. Box 2455, Riyadh 11451, Saudi Arabia

<sup>f</sup> Department of Chemistry and Biochemistry, The Ohio State University, 151 W. Woodruff Ave, Columbus, OH 43210, USA

<sup>g</sup> Biomedical Research Unit and Lab Animal Research Centre, Saveetha Dental College, Saveetha Institute of Medical and Technical Sciences, Chennai 602 105, India

<sup>h</sup> Faculty of Science, Universiti Tunku Abdul Rahman, Kampar 31900, Malaysia

<sup>i</sup> Faculty of Bioeconomics and Health Sciences, Universiti Geomatika Malaysia, Kuala Lumpur 54200, Malaysia

## ARTICLE INFO

### Article history:

Received 24 May 2023

Revised 22 July 2023

Accepted 13 September 2023

Available online 21 September 2023

### Keywords:

Corrosion

Sodium citrate

Binary inhibitor

Super hydrophobicity

Electrochemical studies

## ABSTRACT

In this work, the mixture of trisodium citrate and  $Zn^{2+}$  was used as binary (hetero type) inhibitor for corrosion inhibition of copper metal in potable water. The binary inhibitor system ( $Zn^{2+}$  and trisodium citrate) was used to form hydrophobic surfaces on copper submerged in potable water. Water contact angle (WCA) was found to be  $155^{\circ}$  when the inhibitor was present, whereas it was  $84^{\circ}$  when there was no inhibitor. These observations suggested the development of superhydrophobic layer on the surface of copper in drinkable water. Electrochemical impedance spectroscopy (EIS – AC mode), and potentiodynamic polarization (DC mode) experiments conveyed that the copper surface could be protected by utilizing the mixture of trisodium citrate and  $Zn^{2+}$  in potable water. The morphological studies including SEM (coupled with EDX), AFM, and WCA were evidenced the formulation of a hetero-type inhibitor for the corrosion inhibition of copper in potable water. In this study, the decline in the double-layer capacitance and the rise in the charge transfer resistance were due to the adsorption of inhibitor confirming the development of protective layer, which EIS, SEM, EDX, AFM, and WCA studies also supported. Thus, there was a synergism observed between TSC and  $Zn^{2+}$ , and the formulation consisting of TSC and  $Zn^{2+}$  provided 83% of inhibition efficiency ( $IE_p$ ). So, it was suggested that the approach reported in this study could be a simple method for obtaining the superhydrophobic copper surface.

© 2023 The Author(s). Published by Elsevier B.V. on behalf of King Saud University. This is an open access article under the CC BY-NC-ND license (<http://creativecommons.org/licenses/by-nc-nd/4.0/>).

## 1. Introduction

In common, much attention is not being focused on the plumbing work during a typical water delivery system. Hence, a potential care must be given to such a plumbing system. Generally, there would be no issues due to hidden beneath walls, ceilings, floors,

and cabinets. In contrast, dripping outlets, sticky or leaky toilet tank/pipe valves, and a malfunctioning water heater would frequently lead to residential water issues. Of course, most of the house owners might have encountered these nuisances. Among these, pipe leaks only cause minor water supply concern but might cause significant water problems if not noticed promptly. Corrosion in water pipes is the main reason for these pipe leaks. Water pipe's performance and service life are influenced by several variables, including pipe size, type, permanent piping system design and craftsmanship, level of water environment corrosion, and pipe age (Lyman et al., 1982). As a result, each component must be

\* Corresponding authors.

E-mail addresses: [antarajan@ksu.edu.sa](mailto:antarajan@ksu.edu.sa) (N. Arumugam), [teylh@utar.edu.my](mailto:teylh@utar.edu.my) (L.-H. Tey).

Peer review under responsibility of King Saud University

looked at while assessing the condition or leaking of a home's water pipe system. The pipe that is generally installed inside a home is copper, although it can also be galvanised steel / plastic (CPVC/ PVC or polybutylene) pipe. This section provided basic information for house owners concerning plumbing issues and leaks (Myers and Cohen, 1995). Like any mass-produced device, a copper water tube might have some faults or problems. So, any leakage inquiry must primarily include an inspection of the copper tube. A flaw in a copper tube's wall seldom goes undetected for long. The pressure assessing and commissioning of the plumbing technique will automatically reveal fissures, as-manufactured holes, or other flaws. So, if a house owner has a leakage for days or weeks after installing a system, a material flaw or poorly manufactured fitting connection could likely be blamed. The longer a system runs before a leakage, the more probable reasons would be faulty craftsmanship, insufficient flushing or stagnation, or aggressive water chemistry.

Water contact angle measurement technique is the easy and best way to determine the hydrophobic or hydrophilic environment of the corrosion system, which is responsible for leakage of malfunctioning of water pipelines or plumbing systems. Surface studies can explain the phenomenon of wetting of solid surfaces by liquid. When a droplet of liquid hits a solid substrate, it stays as a droplet or spreads out to create a thin liquid film, which can be measured by water contact angle (CA). If the CA of water or oil on a solid substrate is above 150°, it is superhydrophobic or super-oleophobic where the water or oil droplets bounce off the surface. If water or oil's CA is practically 0°, then the surface is said to be super-hydrophilic or super-oleophilic. In natural systems, even plant leaves, including colocasia esculenta (Taro), nelumbo nucifera (lotus), and brassica oleracea (wild cabbage) (Barthlott and Neinhuis, 1997; Chen et al., 2007; Choi, et al., 2007; Neinhuis and Barthlott, 1997; Koch et al., 2004; Karthick and Maheshwari, 2008; Arvind Singh et al., 2007), water strider legs, and butterfly wings possess this kind of superhydrophobic (Goodwyn et al., 2009; Gao and Jiang, 2004) characteristics. The surface of lotus leaf has micro and or nano epidermal assemblies. They are commonly coated with 100-nanometer wax crystals.

Micro and nanostructures combined with hydrophobic chemistry provide superhydrophobicity in lotus leaf, with CA more than 150° (Spaetha and Barthlott, 2008). Biomimetic super-hydrophobic surfaces are being developed in non-wetting garments, self-cleaning spectacles, anti-snow sticking, monument protection, and corrosion protection coatings (Yin et al., 2008; Liu et al., 2007; Mah and O'Toole, 2001). In this study, we described the creation of a corrosion-resistant hydrophobic protective coating on copper surfaces in potable water. Copper is broadly used in various fields because of its outstanding thermal and electrical conductivity and also due to its good workability. The copper corrosion implies essential economic losses for various industries, and such corrosion phenomenon can be inhibited by using the appropriate inhibitors (Quartarone et al., 2008; Li et al., 2018). Numerous organic and inorganic inhibitors have been developed to prevent copper corrosion (Zhang et al., 2018). However, some of these inhibitors have drawbacks, such as being noxious to humans, high cost, and environmental pollution risk (Raja and Sethuraman, 2008). Hence, researchers have always wanted some alternatives by congregating on low-cost and environmentally friendly biodegradable materials that may not cause any danger to human health and the environment (Fateh et al., 2017; Mo et al., 2016). Thus, this work aimed to evaluate the inhibitory effects of Zn<sup>2+</sup> and eco-friendly trisodium citrate (synergistic effect) on copper corrosion in potable water using electrochemical techniques which could be considered as the novelty of this work. The surface film was also analysed by using surface analytical methods.

## 2. Experimental

### 2.1. Materials

The copper specimens of sizes 1 x 4 cm and 0.2 cm thickness were press cut, machined, and emery-papered. Then, the sample was rinsed with acetone and double distilled water followed by air drying. Prior to the experiment, the substrates were prepared as stated and utilized immediately. Zn<sup>2+</sup> and TSC were utilized as such. A 1000 ppm TSC stock solution was diluted further to prepare the dilute solution of the required concentration. All solutions were made up of the potable water from Perambalur, Tamil Nadu State, India. The investigation was carried out at room temperature. Table 1 shows the physico-chemical parameters of potable water.

### 2.2. Electrochemical studies

The CHI-760D model electrochemical workstation was used for polarisation and EIS tests, and software Version: 12.22.0.0, was used to evaluate the experimental data. The tests were performed via three-electrode glass cell with a saturated calomel reference electrode and a platinum auxiliary electrode. Only 1 cm<sup>2</sup> of the working electrode, which was made of copper and covered in polytetrafluoroethylene epoxy resin, was in contact with the electrolyte. With blank and the presence of inhibitor formulations, the three electrodes were submerged in 100 ml control solution to manage a consistent open circuit potential (OCP). The solutions were not stirred, and the pH was set to 7.0. The schematic diagram of electrochemical setup has been described in supplementary section (vide supplementary data, Fig. S1).

The polarisation curves were obtained from -750 to -150 mV with 2 mV resolution. The curves were acquired in a dynamic scan mode at 2 mV s<sup>-1</sup> in the -20 to +20 mA range. The tests were compensated for Ohmic drop. The extrapolated anodic and cathodic Tafel plots yielded the corrosion current density ( $I_{corr}$ ), corrosion potential ( $E_{corr}$ ), cathodic (c) and anodic (a) as shown in Fig. 1. The  $PE_p$  was calculated from  $I_{corr}$  as shown in the following equation;

$$(\%)PE_p = \frac{I_{corr} - I'_{corr}}{I_{corr}} \times 100$$

$I_{corr}$  and  $I'_{corr}$  are the values of corrosion current densities for blank and inhibited solutions respectively.

EIS results were obtained at OCP with 4 to 10 steps per decade from 60 KHz to 10 MHz. The system was perturbed with 10 mV sine wave. Nyquist plots yielded the charge transfer resistance ( $R_{ct}$ ) curves and double-layer capacitance ( $C_{dl}$ ). The protection efficiency ( $PE_{im}$ ) was calculated as follows;

$$(\%)PE_{im} = \frac{R_{ct} - R'_{ct}}{R'_{ct}} \times 100$$

$R_{ct}$  and  $R'_{ct}$  are the values of the charge transfer resistance for inhibitor and blank respectively.

**Table 1**  
Physico-chemical parameters of potable water.

Parameters	Values
pH	7.84
TDS	251 ppm
Chloride	30 ppm
Alkalinity	113 ppm
Total Hardness	102 ppm
Conductivity	358 $\mu$ mhos/cm

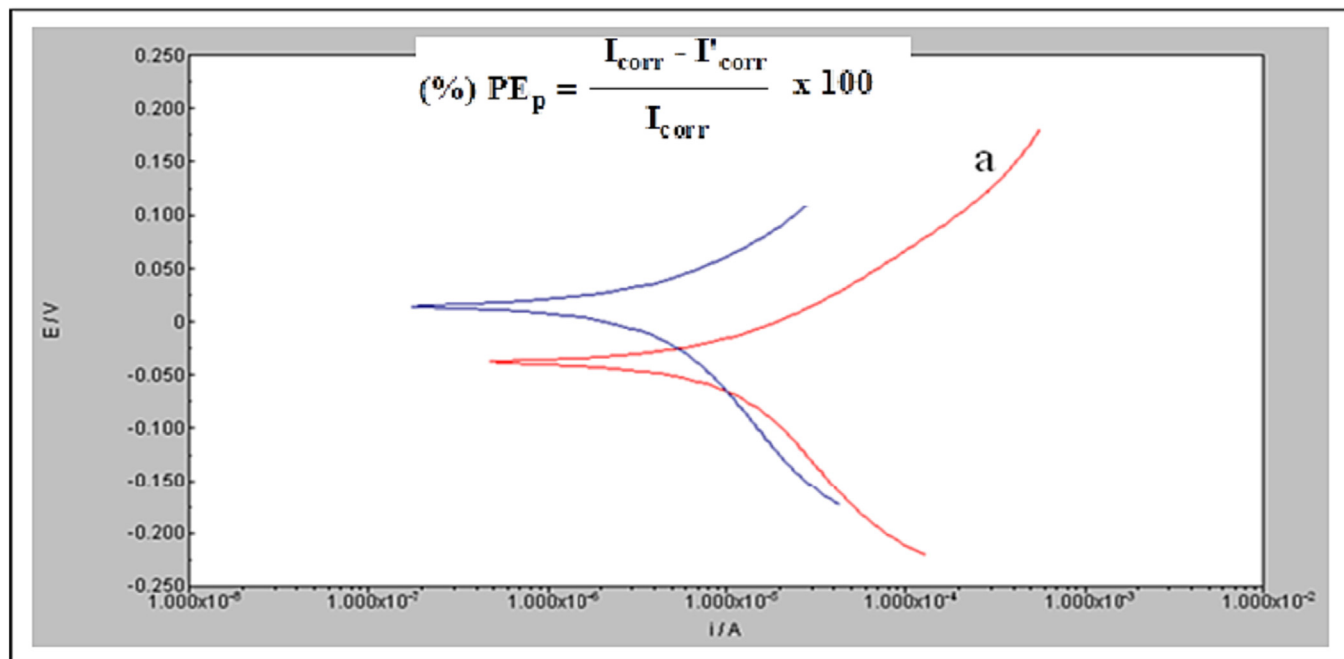


Fig. 1. Tafel plots of copper in potable water (a) blank; (b) with 10 ppm  $Zn^{2+}$ +100 ppm TSC.

### 2.3. SEM

SEM (Model: TESCAN vega3 USA) was used to determine the surface morphology of copper with presence and absence of inhibitors. To explore the surface morphology of copper, the polished specimens were studied under an optical microscope for any surface defects, such as cracks. Only smooth, pit-free specimens were immersed and the immersion lasted for 7 days. After testing, the samples were dried and rinsed with double-distilled (DD) water before SEM analysis.

### 2.4. EDAX

EDAX (BRUKER Nano Germany) was used to screen the protective film produced on the copper surface. As a kind of spectroscopy, it uses electromagnetic radiation to study the samples. X-rays were converted into electrical signals that a detector can detect. The data were delivered to a pulse processor that determined the signs and sent them to an analyzer.

### 2.5. AFM

The copper specimens' surface roughness is measured via atomic force microscopy (AFM). The surface image's resolution and accuracy are improved because to this creative method. AFM was used to scan the protective films and assess the roughness (Dumas et al., 1993). The surface morphological changes at several hundred nanometers caused by corrosion and the formation of protective layers with and without inhibitors, respectively, were directly visible using AFM. The Pico SPM2100 was used to take all AFM images while in air contact mode.

### 2.6. Water contact angle (WCA) technique

Experimentally, the contact angle was measured by using the sessile droplet technique. The sessile droplet was horizontally held in a syringe. A high-resolution camera (10.1 Mpixel SONY camera) was used to capture the image after the substrate was lit. The

image was then processed using the appropriate specialised software.

## 3. Results and discussion

### 3.1. DC – potentiodynamic polarization technique

Table 2 shows the corrosion characteristics of copper obtained from potentiodynamic polarization studies by using Tafel curves. The copper's corrosion potential ( $E_{corr}$ ) was  $-0.038$  mV (Vs SCE), and the respective corrosion current density ( $I_{corr}$ ) was  $6.837 \times 10^{-6}$  A/cm<sup>2</sup> when submerged in potable water. After adding 10 ppm  $Zn^{2+}$  and 100 ppm TSC, the corrosion potential values were increased to 0.038 mV. It was actually an anodic shift with the reduction of corrosion current density, and a (57 mV) was found to be smaller than that of c (76 mV). The results confirmed that it is a hetero (mixed)-type inhibitor, which was in good agreement with the reports (Ferreira et al., 2004; Li et al., 2008; Kasilingam and Thangavelu, 2016; Viswanatham and Halder, 2007). In the presence of  $Zn^{2+}$  and TSC ions, the corrosion potential shifted anodically, and the corrosion current dropped from  $6.837 \times 10^{-6}$  A/cm<sup>2</sup> to  $1.129 \times 10^{-6}$  A/cm<sup>2</sup>. This was due to the reason that the inhibiting layer generated on the metal surface could slow the breakdown of iron. Such passivity of iron was explained due to the formation of TSC- $Fe^{2+}$  surface layer. Thus, this study's significantly lower corrosion current might imply the improved adsorption and efficacy of inhibitors (Gunasekaran and Chauhan, 2004). It was observed when the inhibitors were added 83%  $IE_p$  was obtained. In order to inhibit the development of rust, it was suggested that the creation of  $Zn(OH)_2$  and the building of a protective coating (TSC- $Fe^{2+}$ ) on metal surfaces could be the potential mechanisms. The binary inhibitor formulation was therefore shown to be capable of controlling both the cathodic and anodic processes.

### 3.2. AC – EIS technique

Fig. 2 displays the Nyquist impedance spectra of copper submerged in potable water with the absence (control) and presence of  $Zn^{2+}$  and TSC. The charge transfer resistance ( $R_{ct}$ ), double layer capacitance ( $C_{dl}$ ), and predicted protection efficiency ( $PE_{im}$ ), which

**Table 2**  
Corrosion parameters for copper obtained from potentiodynamic polarization technique with and without inhibitor formulation.

Concentration (ppm)		Tafel parameters				IE <sub>p</sub> (%)
TSC	Zn <sup>2+</sup>	E <sub>corr</sub> mV vs SCE	i <sub>corr</sub> A/cm <sup>2</sup> × 10 <sup>-6</sup>	β <sub>a</sub> mV/decade	β <sub>c</sub> mV/decade	
Blank		- 0.050	6.837	67	119	-
100	10	0.038	1.129	57	76	83

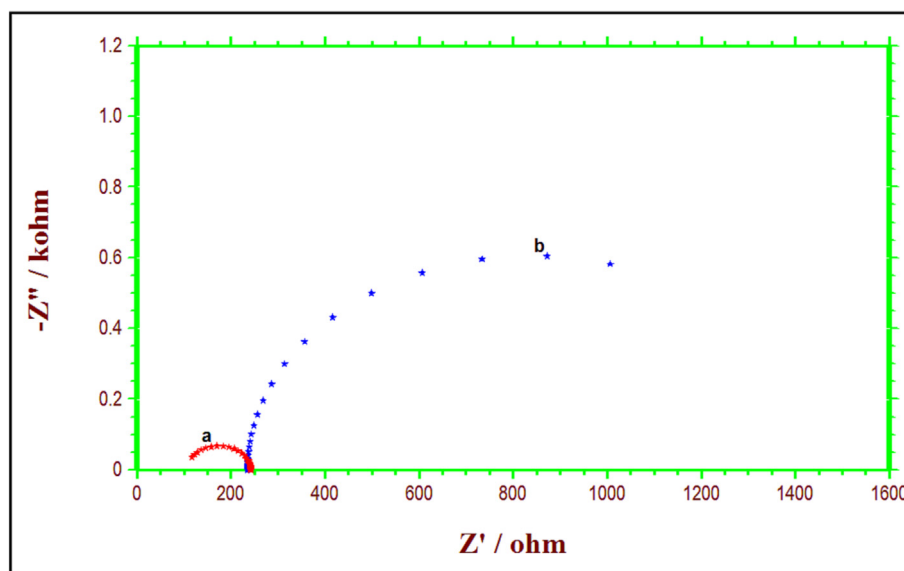


**Fig. 2.** Nyquist plots of copper in potable water (a) blank; (b) with 10 ppm Zn<sup>2+</sup>+100 ppm TSC.

**Table 3**  
Nyquist plots for copper immersed in the potable water obtained by EIS analysis in the absence and presence of inhibitor solution.

Concentration (ppm)	Zn <sup>2+</sup>	Charge transfer Resistance, R <sub>ct</sub> (Ω)	Double layer capacitance, C <sub>dl</sub> CPE μF/cm <sup>2</sup>	IE <sub>im</sub> (%)
Blank		107.09	28.595	-
100	10	940.00	0.360	88

are Nyquist impedance parameters, are provided in Table 3. The data from Nyquist plots are fitted using the analogous electrical circuit, as shown in Fig. 3.

Many researchers (Morad, 2000; Alagta et al., 2007) reported the depressed semicircles with a single-time constant circuit. A constant phase element (CPE), rather than a pure double-layer capacitor, is more typically used. When copper was dissolved in potable water, the R<sub>ct</sub> value was found to be 107.09 and the C<sub>dl</sub> value was 28.595F/cm<sup>2</sup>. By adding 10 ppm of Zn<sup>2+</sup> and 100 ppm of TSC to the blank, Nyquist plots from high to low-frequency directions revealed a sizable, depressed semicircle, revealing that the charge transfer resistance became dominant the corrosion processes as a result of the adsorption of a protective layer onto the copper surface. Also, R<sub>ct</sub> value increased from 107.09 to 940, and C<sub>dl</sub> decreased to 0.360F/cm<sup>2</sup>. Impedance experiments show that a chemical protects drinkable water by increasing R<sub>ct</sub> and decreasing double-layer capacitance. This establishes the film’s existence and formation (Ouchrif et al., 2005).

3.3. Scanning electron microscope (SEM)

SEM micrographs of the surface were investigated to study the composition of the surface layer without inhibitors and the level of

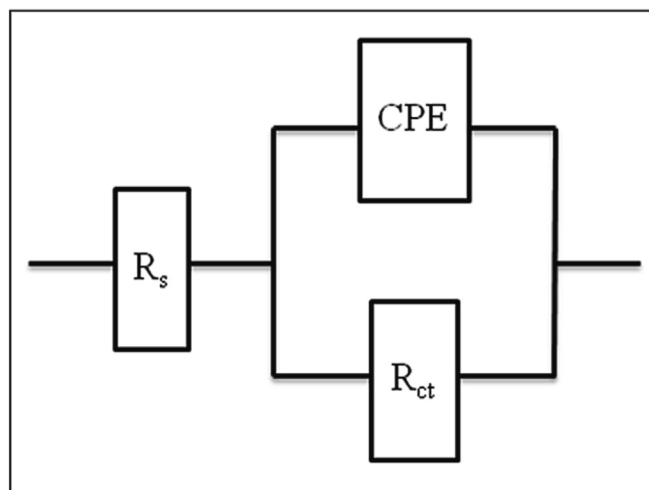


**Fig. 3.** The fitted Nyquist plots by the equivalent electrical circuit.

copper corrosion. The morphology of the samples showed that the inhibitor had a significant impact on the structure of the copper surface. A uniformly dispersed protective coating was produced across the entire surface of the metal which could be seen through the difference in the surface of the samples with and without inhibitors. The inhibitor’s adsorption and subsequent absorption into the passive film inhibited the corrosion active site on the surface of copper, completely encasing the metal in the barrier. Fig. 4 shows SEM images of copper submerged in potable water over seven days with and without an inhibitor. In Fig. 4a, SEM micrographs of copper surface submerged in potable water indicated

that the surface (rough) was significantly corroded, faulting the metallic characteristics and forming the corrosion products without an inhibitor formulation. Both the surface and the corrosion products were unequal. The development of an insoluble complex on the metal's surface (the Zn<sup>2+</sup>-TSC inhibitor) and a thin layer of inhibitor that effectively inhibits copper dissolution are shown in Fig. 4b, which showed that the surface (smooth) coverage enhanced with the presence of 10 ppm of Zn<sup>2+</sup> and 100 ppm of TSC in potable water (Harvath and Kalman, 2000).

### 3.4. EDAX

By using this technique, the percentages of various atoms present in a sample can be calculated. As a result, EDAX also verified the development of a protective coating on the surface of copper. The corrosion phenomenon was depicted in Fig. 5a by the EDAX spectrum of polished copper submerged in potable water without the inhibitor molecules. However, due to the presence of a protective layer of inhibitor molecules on the surface of the copper sam-

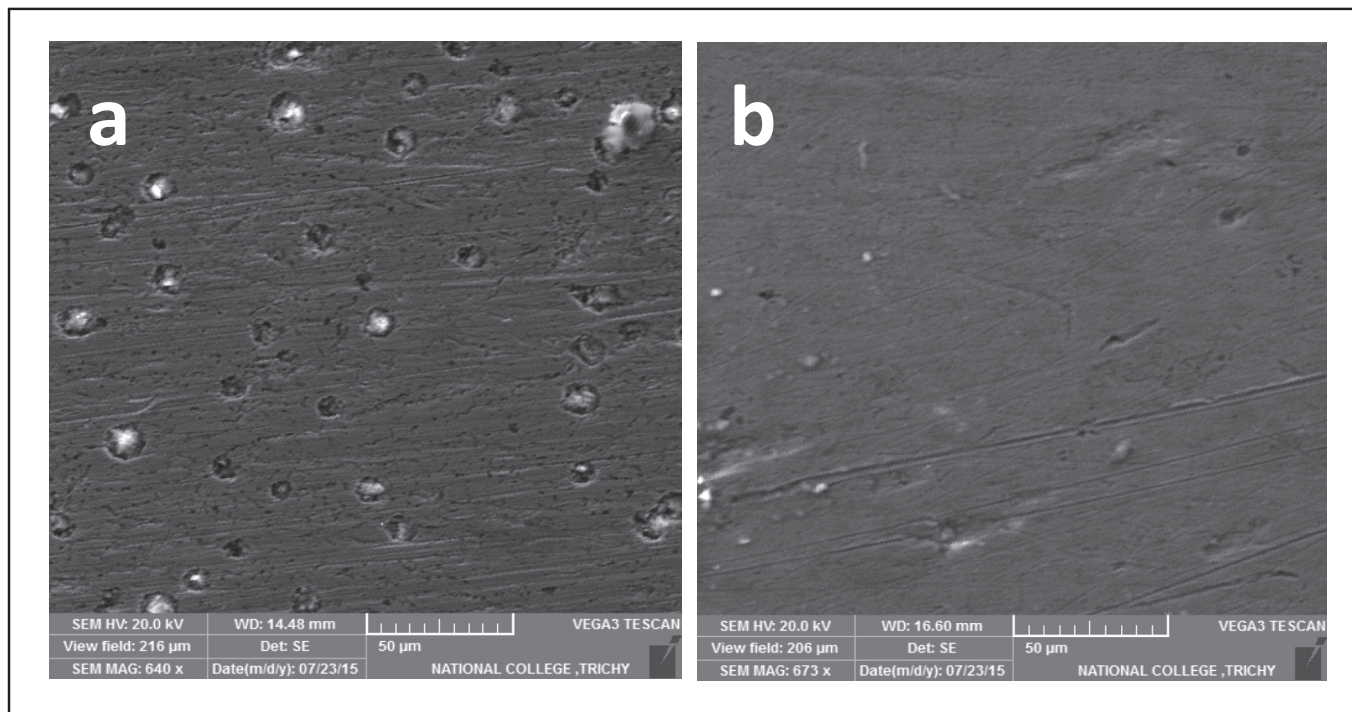


Fig. 4. SEM images of copper in potable water (a) blank; (b) with 10 ppm Zn<sup>2+</sup>+100 ppm TSC.

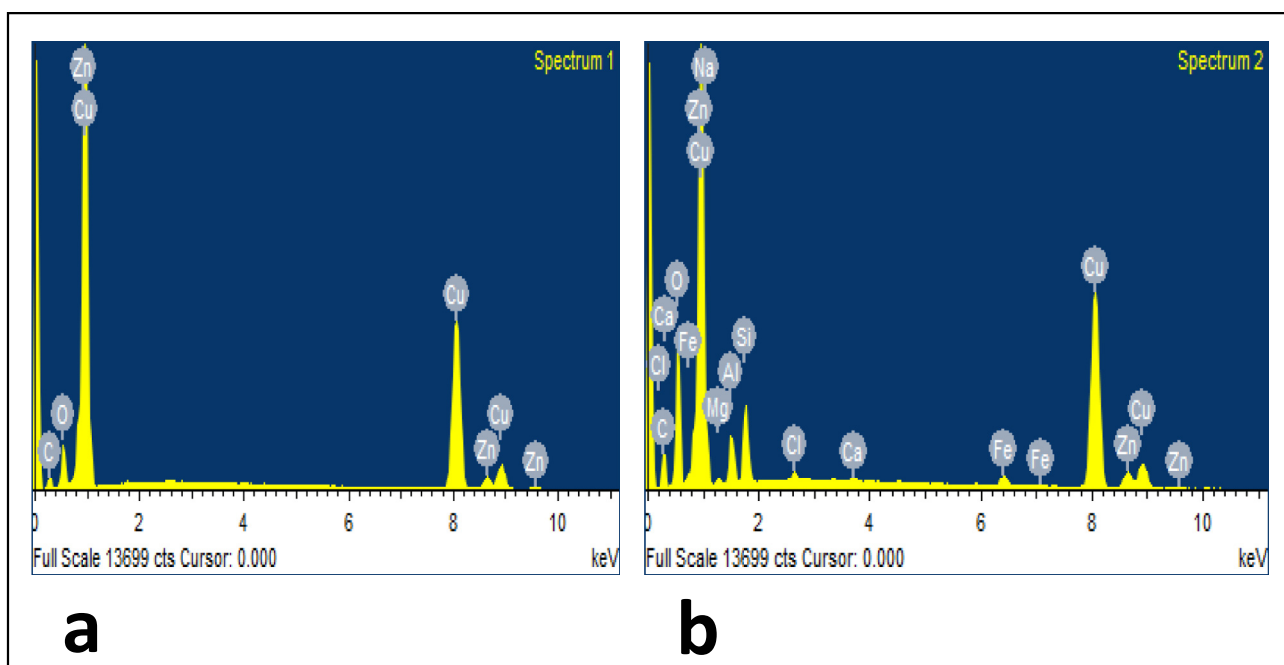


Fig. 5. EDX spectra of copper in potable water (a) blank; (b) with 10 ppm Zn<sup>2+</sup>+100 ppm TSC.

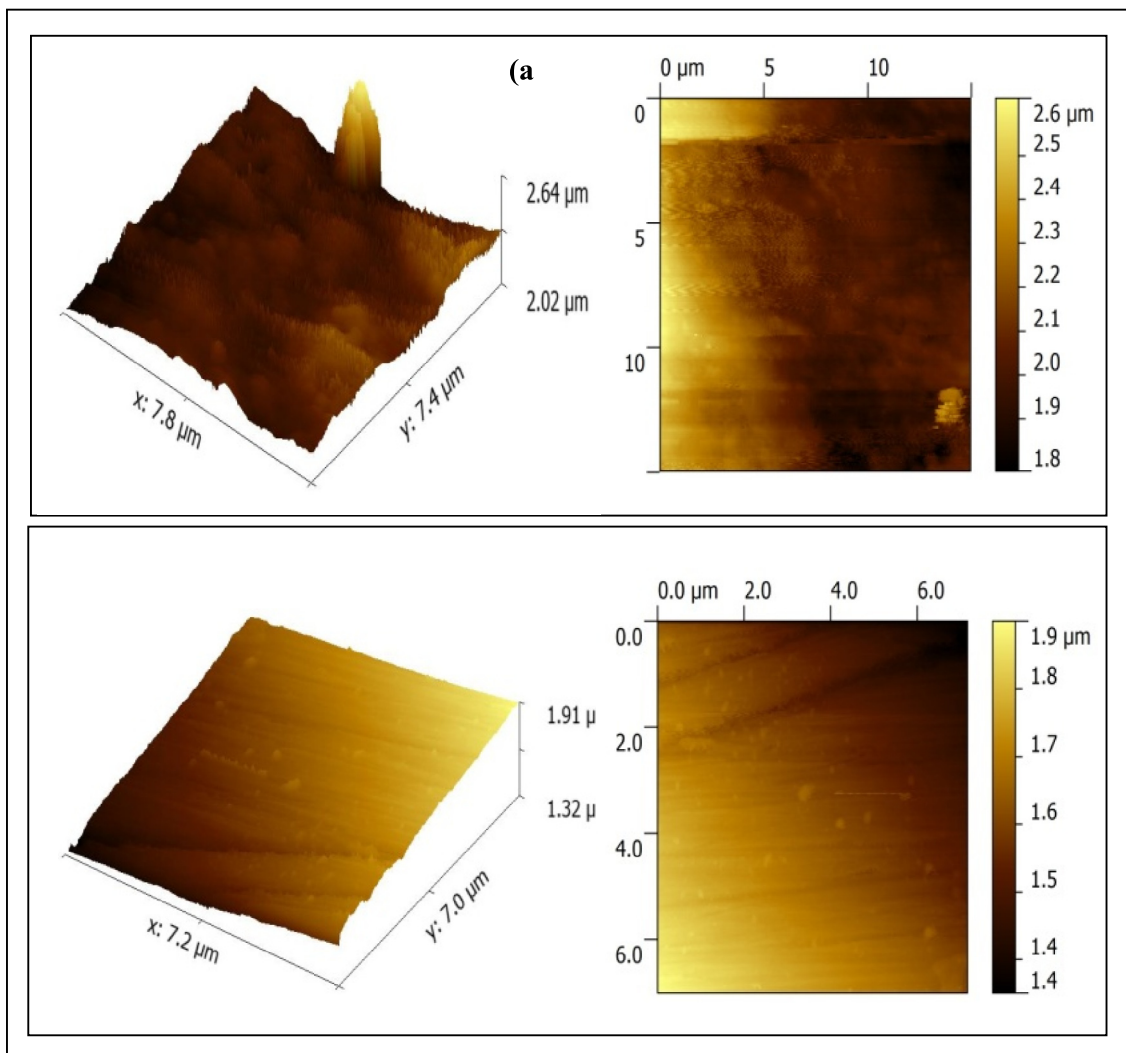


Fig. 6. AFM images of copper in potable water (a) blank; (b) with 100 ppm Zn<sup>2+</sup>+100 ppm TSC.

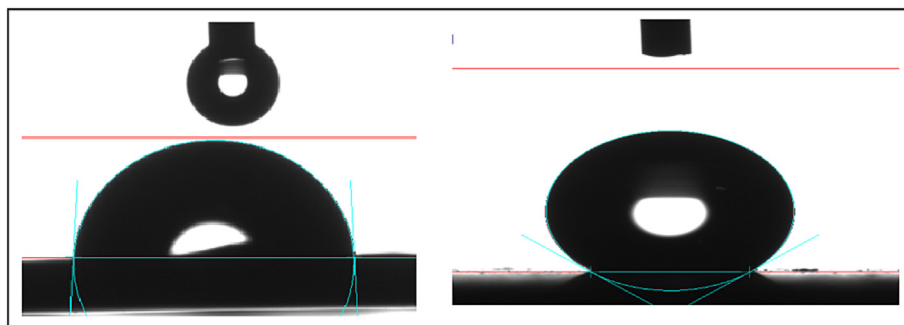


Fig. 7. Water contact angle image of copper surface in potable water (a) blank; (b) with 10 ppm Zn<sup>2+</sup>+100 ppm TSC.

ple, iron, carbon, sodium, oxygen, and zinc peaks appeared in the EDAX spectra upon the addition of 10 ppm Zn<sup>2+</sup> and 100 ppm TSC to the blank as shown in Fig. 5b (Mohanasundaram et al., 2022). The formation of a protective layer coincided with a reduction in the intensity of the metal peaks. The development of this barrier or protective coating may be a result of inhibitors adhering to electrodes.

### 3.5. Atomic force microscope

From AFM images, it is common to derive the average roughness (Ra), root mean square roughness (RMS) roughness (R<sub>q</sub>), and maximum peak-to-valley height. Results from the 2D and 3D AFM on copper in potable water with and without the inhibitor molecules are shown in Fig. 6. From Fig. 6a, the AFM image indi-

cated a rough surface (maximum surface roughness 2.5  $\mu\text{m}$ ) owing to the corrosion of copper in the absence of an inhibitor. In the presence of (10 ppm  $\text{Zn}^{2+}$  and 100 ppm TSC), the copper was less corroded, and the surface was smooth and homogeneous with the different-shaped layer (maximum surface roughness 0.5  $\mu\text{m}$ ) as shown in Fig. 6b. due to the adsorption of the inhibitor on the surface. Thus, the values of average roughness, RMS roughness and peak-to-valley height for the system without inhibitor were greater than that of the system with inhibitor. It was also seen from Fig. 6a that there were some pits on the surface of the copper and from Fig. 6b, it was observed that the height was lower than that of the average depth in some places. Also, in the presence of the inhibitor, the entropy might decrease due to the presence of the protective layer (Praveena et al., 2020). Thus, it could be stated that the metal surface was coated for protection. The decrease in  $R_{\text{RMS}}$  value in the presence of inhibitor) was the indication of increased uniform coating and smoothness, as well as the absence of the deposition of the corrosion product. The variance discovered in the optical cross-section study also supported these findings. Thus, AFM analysis confirmed the formation of a coating on the surface of the metal to shield it from corrosion.

### 3.6. Water contact angle (WCA) measurement technique

The water contact angle was measured as indicated in Fig. 7 to determine the surface's wettability, hydrophobicity, and hydrophilicity. If the inhibitor forms self-assembled monolayers on the metal surface, this is understood. While the contact angle, hydrophobicity, and corrosion inhibition efficiency would all increase, the wettability would decrease (Praveena et al., 2020). Fig. 7a, illustrates the copper surface submerged without inhibitor was very porous, rough, and hydrophilic (contact angle  $84^\circ$ ). Fig. 7b, shows the surface of copper submerged in potable water with the inhibitor formulation (10 ppm  $\text{Zn}^{2+}$ +100 ppm TSC) became smoother and the contact angle of  $154^\circ$  was increased, confirming the superhydrophobic (Sudhakaran et al., 2022) nature of the surface. This was evidence of the superhydrophobic coating of an inhibitor adsorbed on the copper surface.

## 4. Conclusion

This research concluded that the formulation of the inhibitors was a hetero-type mixture of  $\text{Zn}^{2+}$ -TSC that could successfully inhibit copper corrosion in drinking water by creating a protective layer on the surface of copper. According to the potentiodynamic polarisation investigations, the coating was created at the electrode's anodic terminal. The binary inhibitor system might create a shield (coating) over the copper surface/solution contact area, according to the EIS experiments. Investigations using SEM, EDX, and AFM further supported the formulation's development of a protective layer on copper. The super-hydrophobicity of the protective coating was further understood by the measurements of water contact angles.

### Declaration of Competing Interest

The authors declare that they have no known competing financial interests or personal relationships that could have appeared to influence the work reported in this paper.

### Acknowledgement

The project was funded by Researchers Supporting Project number (RSP2023R143), King Saud University, Riyadh, Saudi Arabia.

## Appendix A. Supplementary data

Supplementary data to this article can be found online at <https://doi.org/10.1016/j.jksus.2023.102907>.

## References

- Alagta, A., Felhosi, I., Teleghi, J., Bertóti, M., Kálmán, E., 2007. Effect of metal ions on corrosion inhibition of pimeloyl-1,5-di-hydroxamic acid for steel in neutral solution. *Corros. Sci.* 49, 2754–2766.
- Arvind Singh, R., Yoon, E.-S., Kim, H.J., Kim, J., Jeong, H.E., Suh, K.Y., 2007. Replication of surfaces of natural leaves for enhanced micro-scale tribological property. *Mater. Sci. Eng. C* 27, 875–879.
- Barthlott, W., Neinhuis, C., 1997. Purity of the sacred lotus, or escape from contamination in biological surfaces. *Planta* 207, 1–8.
- Chen, C.-H., Cai, Q., Tsai, C., Chen, C.-L., Xiong, G., Yu, Y., Ren, Z., 2007. Dropwise condensation on superhydrophobic surfaces with two-tier roughness. *Appl. Phys. Lett.* 2007, (90) 173108.
- Choi, C.H., Hagvall, S.H., Wu, B.M., Dunn, J.C.Y., Beygui, R.E., Kim, C.-J., 2007. Cell interaction with three-dimensional sharp-tip nanotopography. *Biomaterials* 28, 1672–1679.
- Dumas, P., Buttikhreddine, B., Amra, C., Vatel, O., Andre, E., Galindo, R., Salvan, F., 1993. Quantitative microroughness analysis down to the nanometer scale. *Europhys. Lett.* 22, 717–722.
- Fateh, A., Aliofkhaezai, M., Rezvani, A.R., 2017. Review of corrosive environments for copper and its corrosion inhibitors. *Arab. J. Chem.* 13, 481–544.
- Ferreira, E.S., Giacomellic, C., Giacomellic, F.C., Spinelli, A., 2004. Evaluation of the inhibitor effect of L-ascorbic acid on the corrosion of mild steel. *Mater. Chem. Phys.* 83, 129–134.
- Gao, X., Jiang, L., 2004. Water-repellent legs of water striders. *Nature* 432, 36.
- Goodwyn, P.P., Maezono, Y., Hosoda, N., Fujiseki, K., 2009. Waterproof and translucent wings at the same time: problems and solutions in butterflys. *Naturwissenschaften*, 781–787.
- Gunasekaran, G., Chauhan, L.R., 2004. Eco-friendly inhibitor for corrosion inhibition of mild steel in phosphoric acid medium. *Electrochim. Acta* 49, 4387.
- Harvath, T., Kalman, E., 2000. Study of corrosion inhibition phenomena in acidic media by electrochemical and surface analysis techniques. *Russ. J. Electrochem.* 36, 1085–1091.
- Karthick, B., Maheshwari, R., 2008. Lotus-inspired nanotechnology applications. *Resonance* 13, 1141–1145p.
- Kasilingam, T., Thangavelu, C., 2016. Biocidal behaviour of (dodecyltrimethylammonium bromide) on carbon steel in well water. *Trans. Indian Inst. Met.* 69, 793–803.
- Koch, K., Neinhuis, N., Ensikat, H.J., Barthlott, W., 2004. Self-assembly of epicuticular waxes on living plant surfaces imaged by atomic force microscopy (AFM). *J. Exp. Bot.* 55, 711–718.
- Li, W.-H., He, Q., Zhang, S.-T., Pei, C.-L., Huo, B.-R., 2008. Some new triazole derivatives as inhibitors for mild steel corrosion in acidic medium. *J. Appl. Electrochem.* 38, 289–295.
- Li, H., Zhang, S., Tan, B., Qiang, Y., Li, W., Chen, S., Guo, L., 2018. Investigation of Losartan Potassium as an eco-friendly corrosion inhibitor for copper in 0.5M  $\text{H}_2\text{SO}_4$ . *J. Mol. Liq.* <https://doi.org/10.1016/j.molliq.2020.112789>.
- Liu, T., Chen, S., Cheng, S., Tian, J., Chang, X., Yin, Y., 2007. Corrosion behavior of super-hydrophobic surface on copper in seawater. *Electrochim. Acta* 52, 8003–8007.
- Lyman, W.S., Cohen, A., Myers, J.R., 1982. Causes and Prevention of Pitting Corrosion in Copper Plumbing Systems in the USA. In: Proceedings of the International Symposium on Corrosion of Copper and Copper Alloys in Buildings. March; Tokyo, Japan.
- Mah, T.-F.-C., O'Toole, G.A., 2001. Mechanisms of biofilm resistance to antimicrobial agents. *Trends Microbiol.* 9, 34–39.
- Mo, S., Luo, H.-Q., Li, N.-B., 2016. Plant extracts as “green” corrosion inhibitors for steel in sulphuric acid. *Chem. Pap.* <https://doi.org/10.1515/chempap.2016.0055>.
- Mohanandaram, S., Ramirez-Asis, E., Quispe-Talla, A., Bhat, M.W., Shabaz, M., 2022. Experimental replacement of hops by mango in beer: production and comparison of total phenolics, flavonoids, minerals, carbohydrates, proteins and toxic substances. *Int. J. Syst. Assur. Eng. Manag.* 13, 132–145.
- Morad, M.S., 2000. An electrochemical study on the inhibiting action of some organic phosphonium compounds on the corrosion of mild steel in aerated acid solutions. *Corros. Sci.* 42, 1307–1326.
- Myers, J.R., Cohen, A., 1995. Pitting Corrosion of Copper in Cold Potable Water Systems. *Materials Performance*. October 60–62p.
- Neinhuis, C., Barthlott, W., 1997. Characterization and distribution of water-repellent, self-cleaning plant surfaces. *Ann. Bot.* 79, 667–677.
- Ouchrif, A., Zegmout, M., Hammouti, B., El-Kadiri, S., Ramdani, A., 2005. 1,3-bis(3-hydroxymethyl-5-methyl-1-pyrazole) propane as corrosion inhibitor for steel in 0.5 M  $\text{H}_2\text{SO}_4$  solution. *Appl. Surf. Sci.* 252, 339–344.
- Praveena, J.M., Rathish, R.J., Rajendran, S., Senthil Kumaran, S., Singh, G., Al-Hashem, A., 2020. Chapter 7 - Corrosion inhibition by self-assembling nanofilms. *Corrosion Protection at the Nanoscale: Nanoscale Micro and Nano Technology*. 107–125.

- Quartarone, G., Battilana, M., Bonaldo, L., Tortato, T., 2008. Investigation of the inhibition effect of indole-3-carboxylic acid on the copper corrosion in 0.5M H<sub>2</sub>SO<sub>4</sub>. *Corros. Sci.* 50, 3467–3474.
- Raja, P.B., Sethuraman, M.G., 2008. Natural products as corrosion inhibitor for metals in corrosive media – a review. *Mater. Lett.* 62, 113–116.
- Spaetha, M., Barthlott, W., 2008. Lotus-effect: biomimetic super-hydrophobic surfaces and their application. *Adv. Sci. Technol.* 60, 38–46.
- Sudhakaran, R., Deepa, T., Asokan, T., Govindaraj, M., Kasilingam, T., Babu, S., Sivarajan, A., 2022. Sodium gluconate as corrosion inhibitor for copper in potable water. *Bull. Environment. Pharmacol. Life Sci.* 1, 486–493.
- Viswanatham, S., Halder, N., 2007. Corrosion inhibition of N80 steel in hydrochloric acid by phenol derivatives. *Ind. J. Chem. Technol.* 14, 501–506.
- Yin, Y., Liu, T., Chen, S., Liu, T., Cheng, S., 2008. Structure stability and corrosion inhibition of super-hydrophobic film on aluminum in seawater. *Appl. Surf. Sci.* 255, 2978–2984.
- Zhang, J., Zhang, L., Tao, G., 2018. A novel and high-efficiency inhibitor of 5-(4-methoxyphenyl)-3h-1,2-dithiole-3-thione for copper corrosion inhibition in sulfuric acid at different temperatures. *J. Mol. Liq.* 272, 369–379.